JOURNAL OF THEORETICAL AND APPLIED MECHANICS
45, 4, pp. 753-771, Warsaw 2007

STRESSES OF HARD COATING UNDER SLIDING CONTACT

Roman Kulchytsky-Zhyhailo
Gabriel Rogowski

Bialystok University of Technology, Faculty of Mechanical Engineering, Bialystok, Poland
e-mail: ksh@pb.edu.pl

The two-dimensional contact problem of elasticity connected with an indentation of a rigid cylinder in an elastic semi-space covered by an elastic layer is considered. The detailed analysis of the stress distribution produced by contact pressures and tangential forces is presented. The obtained results for stresses are compared with ones obtained within the framework of theory of elasticity for a half-space loaded by the Hertz pressure.

Key words: hard coatings, contact problem, friction

1. Introduction

The two-dimensional contact problem concerned with the pressing of a rigid cylinder in an elastic half-space which was coated with a layer of a different elastic material, was considered by Gupta *et al.* (1973) and Gupta and Walowit (1974). The authors conducted detailed analysis of the influence of parameters $h = H/a$ (H is the thickness of the layer, a is the half-width of the contact zone) and E_0/E_1 (E_0, E_1 are Young's moduli of the layer and the substrate, respectively) on basic contact characteristics (the contact width and distribution of the contact pressure). Wide employments of hard top layers for the improvement of tribological properties are observed in last years, and they restored the great interest to investigations of the field of stresses responsible for destruction of layers, and namely, for fracture of coatings (cohesive failure) or delamination and spalling (adhesive failure) at the coating/substrate interface. It is shown that fundamental factors responsible for destruction of layers are: maximum tensile stress, which was considered by Gupta *et al.* (1973), Diao

et al. (1994), Anderson and Collins (1995), Houmid Bennani and Takadoum (1999), Schwarzer (2000), Kato (2000), Bargallini *et al.* (2003), Bhomwick *et al.* (2003) and Xie and Tong (2005); the maximum shear stress, considered by Kouitat Nijwa and von Stebut (1999) and Bhomwick *et al.* (2003) (or Huber–Mises reduced stress – the approach used by Anderson and Collins (1995), Kouitat Nijwa *et al.* (1998), Diao (1999), Elsharkawy (1999) and Schwarzer (2000)) and the maximum shear stress at the coating/substrate interface, considered among others by Gupta *et al.* (1973) and Xie and Tong (2005). Therefore, the analysis of such stresses is very important.

In majority of studies, when analysis of stresses in a layer due to contact loads is considered, two hypotheses are accepted: (1) tangential forces working in the area of contact as a result of friction have negligible influence on the distribution of contact pressure, (2) the actual pressure distribution are replaced by Hertz's distribution. In the case, when the first theory does not raise doubts, which was given by Johnson (1985) and Elsharkawy and Hamrock (1993), the second one seems undisputed in the case of very "thin" ($h < 0.2$) or "thick" ($h > 0.7$) coatings. As it is known from Gupta and Walowit (1974), the distribution of contact pressure may considerably differ due to Hertz's distribution. The largest differences among these distributions occur when $0.3 < h < 0.6$. In the case of $h = 0.4$ and $E_0/E_1 > 5$, the maximum value of the contact pressure is not in the centre of the contact area but in some distance from the centre.

In the present work, we will focus on detailed analysis of the stress distribution produced by contact pressure described by Gupta and Walowit (1974) and related tangential forces. We make a comparison between stress fields created by the distribution given by Gupta and Walowit (1974) and Hertz's distribution. It permits one to define conditions in which the replacement of the contact stress distribution presented by Gupta and Walowit (1974) with Hertz's distribution provides results satisfying for engineering practice. We propose a simplified algorithm for solving the contact problem together with the classical algorithm. This algorithm allows one to obtain a formula for pressure calculation which simplifies the analysis of stress fields by direct numerical methods (finite element method or boundary element method).

2. Problem formulation

The problem of an elastic half-space covered by an elastic layer in which a rigid cylinder is pressured, is considered. We assume that the cylinder is in the state

of limit equilibrium (problem A, Fig. 1a) or it slides along the boundary surface of the half-space (problem B, Fig. 1b).

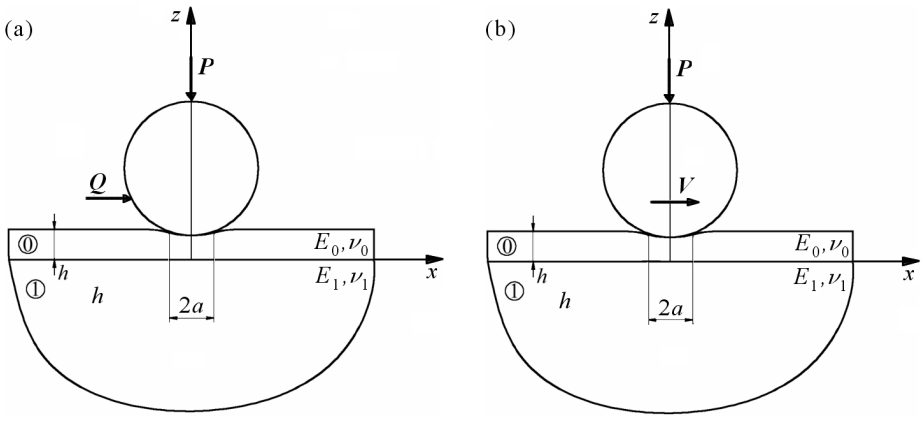

Fig. 1. A scheme of problem I (a) and of problem II (b)

From the mathematical point of view, boundary conditions, typical for the problem of a cylinder sliding along a boundary surface of an elastic half-space with a constant velocity, are the same as the boundary conditions typical for the problem of limit equilibrium. The field of displacements satisfies quasi-static equations of elasticity in movable coordinates. In these coordinates, the z-axis changes its position with constant velocity (the case of a two-dimensional problem was presented by Galin, 1980). On the basis of the solution to the problems connected with loading of the half-space surface by movable pressures (see by Eason, 1965), we can infer that when the velocity of the loading is much lower than the velocity of transverse waves in the considered elastic media, quasi-static equations can replaced by equations of the static theory of elasticity. In engineering calculations, we can obtain that the solution to the contact problem concerned with the limit equilibrium is also the solution to the sliding problem.

We take into account that the height of the cylinder as well as its radius R are much larger than the width of the area of contact $2a$. This approach permits one to consider this problem within the plane state of strain and to approximate the surface of the cylinder by a paraboloid

$$z(x) = \frac{ax^2}{2R} \tag{2.1}$$

where x, z are dimensionless Cartesian coordinates referred to the half-width of the contact. Let us consider that the tangential forces coincident with fric-

tion in the contact region are connected with contact pressure by Amonton's law

$$q(x) = fp(x) \tag{2.2}$$

where f is the coefficient of friction.

Simultaneously, we assume that the tangential forces exert a negligible influence on the size of the contact area and on the distribution of contact pressure described by Johnson (1985). The ideal mechanical contact conditions between the layer and the half-space are assumed.

All state functions denoted by the upper index 0 describe the state of displacement and stresses in the layer; the state functions for the elastic half-space are denoted by the index 1 (E is Young's modulus, ν – Poisson's ratio).

We seek the final solution as a sum of two solutions. The first one is the solution to the contact problem (problem I), while the second one stands for the solution to the problem of elasticity for the half-space loaded by tangential forces on the boundary (problem II). In these problems, the equations of the elasticity theory should be satisfied

$$\begin{aligned} (1-2\nu_i)\Delta u_x^{(i)} + \frac{\partial \theta_i}{\partial x} &= 0 \\ (1-2\nu_i)\Delta u_z^{(i)} + \frac{\partial \theta_i}{\partial z} &= 0 \end{aligned} \qquad i = 0, 1 \tag{2.3}$$

and boundary conditions

$$\begin{aligned} &u_x^{(0)} = u_x^{(1)} \qquad u_z^{(0)} = u_z^{(1)} \qquad \sigma_{xz}^{(0)} = \sigma_{xz}^{(1)} \\ &\sigma_{zz}^{(0)} = \sigma_{zz}^{(1)} \qquad z = 0 \end{aligned} \tag{2.4}$$

— problem I

$$\sigma_{xz}^{(0)} = 0 \qquad \sigma_{zz}^{(0)} = -p(x)H(1-x^2) \qquad z = h \tag{2.5}$$

— problem II

$$\sigma_{xz}^{(0)} = fp(x)H(1-x^2) \qquad \sigma_{zz}^{(0)} = 0 \qquad z = h \tag{2.6}$$

and

$$\sigma_{ij}^{(1)} \to 0 \qquad x^2 + z^2 \to \infty \tag{2.7}$$

where $\boldsymbol{u}$ is the vector of the non-dimensional displacement referred to the half-width of contact, $\boldsymbol{\sigma}$ is the stress tensor, p is an unknown contact pressure, $H(x)$ is the Heaviside unit step function. The unknown contact pressure should

satisfy the boundary conditions connected with the shape of the pressured cylinder

$$\frac{\partial u_z^{(0)}}{\partial x} = \frac{ax}{R} \qquad -1 < x < 1 \qquad z = h \tag{2.8}$$

and the equilibrium condition:

$$2a \int_0^1 p(x)\, dx = P \tag{2.9}$$

where P is the total normal load, see Fig. 1.

3. The method of solution

The general solution to the system of equations (2.3), which satisfies the regularity conditions in infinity (2.7) presented in the Fourier transform space

$$\widetilde{f}(s,z) = F[f(x,z);\ x \to s] \equiv \frac{1}{\sqrt{2\pi}} \int_{-\infty}^{\infty} f(x,z) \exp(-\mathrm{i}xs)\, dx \tag{3.1}$$

can be written in the form:
— for $0 \leqslant z \leqslant h$

$$\begin{aligned} 2\mathrm{i}s\widetilde{u}_x^{(0)}(s,z) &= a_3(s)[(2+d_0)\sinh(|s|(h-z)) + d_0(h-z)|s|\cosh(|s|(h-z))] + \\ &+ a_4(s)[(2+d_0)\cosh(|s|(h-z)) + d_0(h-z)|s|\sinh(|s|(h-z))] + \\ &+ 2a_5(s)|s|\cosh(|s|(h-z)) + 2a_6(s)|s|\sinh(|s|(h-z)) \\ 2\widetilde{u}_z^{(0)}(s,z) &= d_0(h-z)a_3(s)\sinh(|s|(h-z)) + d_0(h-z)a_4(s)\cosh(|s|(h-z)) + \\ &+ 2a_5(s)\sinh(|s|(h-z)) + 2a_6(s)\cosh(|s|(h-z)) \end{aligned} \tag{3.2}$$

— for $z \leqslant 0$

$$\begin{aligned} 2\mathrm{i}s\widetilde{u}_x^{(1)}(s,z) &= -a_1(s)(2+d_1+d_1|s|z)\exp(|s|z) - 2a_2(s)|s|\exp(|s|z) \\ 2\widetilde{u}_z^{(1)}(s,z) &= d_1 a_1(s) z \exp(|s|z) + 2a_2(s)\exp(|s|z) \end{aligned} \tag{3.3}$$

and

— for $0 \leqslant z \leqslant h$

$$\widetilde{\sigma}^{(0)}_{xx}(s,z)\frac{1}{\mu_0} = a_3(s)[(2d_0+1)\sinh(|s|(h-z)) + d_0(h-z)|s|\cosh(|s|(h-z))] +$$
$$+a_4(s)[(2d_0+1)\cosh(|s|(h-z)) + d_0(h-z)|s|\sinh(|s|(h-z))] +$$
$$+2a_5(s)|s|\cosh(|s|(h-z)) + 2a_6(s)|s|\sinh(|s|(h-z))$$

$$\widetilde{\sigma}^{(0)}_{zz}(s,z)\frac{1}{\mu_0} = -a_3(s)[\sinh(|s|(h-z)) + d_0(h-z)|s|\cosh(|s|(h-z))] -$$
$$-a_4(s)[\cosh(|s|(h-z)) + d_0(h-z)|s|\sinh(|s|(h-z))] - \qquad (3.4)$$
$$-2a_5(s)|s|\cosh(|s|(h-z)) - 2a_6(s)|s|\sinh(|s|(h-z))$$

$$\mathrm{i}\,\mathrm{sgn}\,(s)\widetilde{\sigma}^{(0)}_{xz}(s,z)\frac{1}{\mu_0} =$$
$$= -a_3(s)[(1+d_0)\cosh(|s|(h-z)) + d_0(h-z)|s|\sinh(|s|(h-z))] -$$
$$-a_4(s)[(1+d_0)\sinh(|s|(h-z)) + d_0(h-z)|s|\cosh(|s|(h-z))] -$$
$$-2a_5(s)|s|\sinh(|s|(h-z)) - 2a_6(s)|s|\cosh(|s|(h-z))$$

— for $z \leqslant 0$

$$\widetilde{\sigma}^{(1)}_{xx}(s,z)\frac{1}{\mu_1} = -(2d_1+1+d_1|s|z)a_1(s)\exp(|s|z) - 2a_2(s)|s|\exp(|s|z)$$

$$\widetilde{\sigma}^{(1)}_{zz}(s,z)\frac{1}{\mu_1} = a_1(s)(1+d_1|s|z)\exp(|s|z) + 2a_2(s)|s|\exp(|s|z) \qquad (3.5)$$

$$\mathrm{i}\,\mathrm{sgn}\,(s)\widetilde{\sigma}^{(1)}_{xz}(s,z)\frac{1}{\mu_1} = -a_1(s)(1+d_1+d_1|s|z)\exp(|s|z) - 2a_2(s)|s|\exp(|s|z)$$

where $d_i = 1/(1-2\nu_i)$, $i = 0,1$. Equations (3.2)-(3.5) contain six unknown functions $a_i(s)$, $i = 1,2,\ldots,6$.

These functions are obtained as a solution to linear equations (see Appendix A), satisfying boundary conditions (2.4) and (2.5) (problem I) or (2.4) and (2.6) (problem II). Satisfying boundary condition (2.8) for problem I, we obtain the following integral equation

$$\int_0^1 p^*(y)K(x,y)\,dy = -2(1-\nu_0)a_0^2 x \qquad 0 \leqslant x \leqslant 1 \qquad (3.6)$$

where

$$K(x,y) = \int_0^\infty s\overline{a}_6(s)\cos(sy)\sin(sx)\,ds$$
$$a_6(s) = \frac{1}{\mu_0}\widetilde{p}(s)\overline{a}_6(s) \qquad p(x) = p_0 p^*(x) \qquad a = a_H a_0 \qquad (3.7)$$

$p_0 = P/2a$ is the mean contact pressure, a_H is the Hertzian half-width of contact for the homogeneous half-space with mechanical properties adequate for the layer. The solution to the integral equation is sought in the form

$$p^*(x) = \sum_{i=1}^{m} p_i \sqrt{a_i^2 - x^2} H(a_i^2 - x^2) \tag{3.8}$$

where p_i are unknown parameters, a_i are points within interval $[0,1]$ which are calculated from:

$$a_i = \frac{i(2 + c(2m - i - 1))}{m(2 + c(m-1))} \qquad i = 0, 1, \ldots, m \tag{3.9}$$

Equation (3.9) is taken in such a for so that for $c > 0$ we obtain a partition of the interval $[0,1]$, which condenses in the vicinity of the right end of the interval. Substituting Eq. (3.8) into integral (3.6) and comparing the left and right hand sides in points $x_j = (a_j + a_{j-1})/2$, $j = 1, 2, \ldots, m$, we obtain m linear algebraic equations containing $(m+1)$ unknown parameters p_i, $i = 1, 2, \ldots, m$ and a_0

$$\sum_{i=1}^{m} A_{ji} p_i = -2(1 - \nu_0) a_0^2 x_j \tag{3.10}$$

where

$$A_{ji} = \frac{\pi}{2} a_i \int_0^{\infty} \overline{a}_6(s) \sin(s x_j) J_1(s a_i)\, ds \tag{3.11}$$

The missing $(m+1)$-th equation

$$\frac{\pi}{4} \sum_{i=1}^{m} p_i a_i^2 = 1 \tag{3.12}$$

is found by satisfying equilibrium condition (2.9). The solution to the system of equations is obtained by making use of a numerical method. The results are compatible with those given by Gupta and Walowit (1974).

4. A simplificed algorithm for solving the contact problem

The distribution of contact pressure is sought in the form

$$p^*(x) = \Big[\widehat{p} + \frac{16}{\pi}\Big(1 - \frac{\pi}{4}\widehat{p}\Big) x^2\Big] \sqrt{1 - x^2} \tag{4.1}$$

which satisfies equilibrium condition (2.9). It is necessary to point out that the parameter $\widehat{p}$ is the ratio of the contact pressure in the centre of the contact area to the mean contact pressure. Contact boundary condition (2.8) is replaced by the following conditions

$$u_z^{(0)}(1,h) - u_z^{(0)}(0,h) = \frac{a}{2R} \qquad \int_0^1 [u_z^{(0)}(x,h) - u_z^{(0)}(0,h)]\, dx = \frac{a}{6R} \quad (4.2)$$

Substituting Eq. (4.1) into Eqs. (4.2), we obtain two equations for two unknown parameters

$$(1-\nu_0)a_0^2 + A_i\widehat{p} = B_i \qquad i = 1,2 \quad (4.3)$$

The forms A_i and B_i, $i = 1,2$ are presented in Appendix B.

Figures 2 and 3 show that the solution to the system of equations (4.3) is well approximated by integral equation (3.6). The largest differences among the solutions appear in the case of "thin" layers. They increase together with an enlargement of the ratio of the layer and Young's moduli of substrates. The error of estimation of the half-width of contact for $h = 0.1$ and $E_0/E_1 = 8$ is equal to 3.1%. Accuracy of contact pressure distributions is satisfactory for $h > 0.2$. The largest differences between contact pressure distributions for our contact problem and Hertz's pressure occurs when $h \in [0.3, 0.6]$. In this range, we can use an approximate solution given in Eq. (4.1).

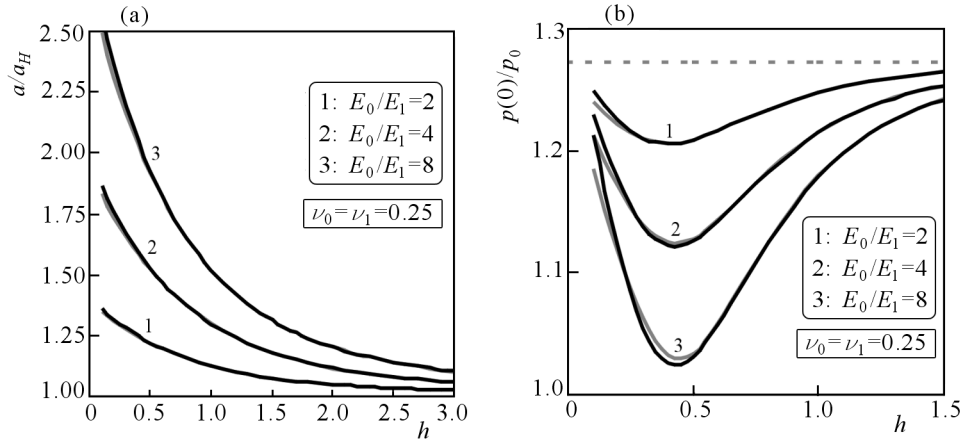

Fig. 2. (a) Non-dimensional half-width of contact. (b) Pressure in the centre of the contact area as functions of the parameter E_0/E_1 (solution to integral equation (3.6) – gray curves, approximate solution – black curves, Hertz solution – dashed curve)

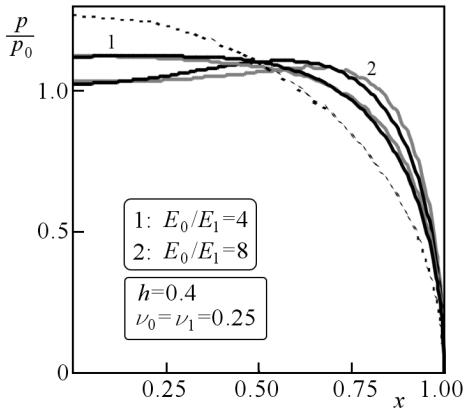

Fig. 3. Distribution of contact pressure (solution of integral equation (3.6) – gray curves, approximate solution – black curves, Hertz solution – dashed curve)

5. The calculation algorithm for stress tensor components

Stress tensor components in interior points of the non-homogeneous half-space can be obtained by numerical calculation of the integrals

$$\sigma_{jk}^{(i)}(x,z) = \frac{1}{\sqrt{2\pi}} \int\limits_{-\infty}^{\infty} \widetilde{\sigma}_{jk}^{(i)}(s,z) \exp(\mathrm{i}xs)\, ds \qquad \begin{matrix} jk = xx, zz, xz \\ i = 0, 1 \end{matrix} \tag{5.1}$$

where the Fourier transforms $\widetilde{\sigma}_{jk}^{(i)}(s,z)$ are described by Eqs (3.4) and (3.5). The accuracy of calculation of integrals (5.1) is supported by the continuity of stresses for $z \to h$. The stresses $\sigma_{xz}^{(0)}(x,h)$ and $\sigma_{zz}^{(0)}(x,h)$ on the surface of the non-homogeneous half-space are known from the boundary conditions. The formula for calculating the stress $\sigma_{xx}^{(0)}(x,h)$ is obtained taking into account the sixth equation of the system of (A1):

$$\sigma_{xx}^{(0)}(x,h) = p(x) + \frac{2\sqrt{2}d_0}{\sqrt{\pi}} \int\limits_{0}^{\infty} [\overline{a}_4(s)\cos(sx) + f\widehat{a}_4(s)\sin(sx)]\widetilde{p}(s)\, ds \tag{5.2}$$

where the relationship $f\widehat{a}_4(s)\widetilde{p}(s) = \mu_0 a_4(s)\mathrm{i}\,\mathrm{sgn}\,(s)$ occurs in problem II.

Asymptotic analysis of the solution to the system of equations (A1) for $s \to \infty$ shows that

$$\overline{a}_4(s) = -\frac{1}{d_0} + \overline{a}_4^*(s) \qquad \widehat{a}_4(s) = -\frac{1}{d_0} + \widehat{a}_4^*(s)$$
$$\lim_{s\to\infty} \overline{a}_4^*(s) = \lim_{s\to\infty} \widehat{a}_4^*(s) = 0 \tag{5.3}$$

Taking into consideration Eq. (5.3), we can write expression (5.2) in the following form

$$\sigma_{xx}^{(0)}(x,h)\frac{1}{p_0} = -p^*(x) - \frac{2\sqrt{2}f}{\sqrt{\pi}}\int_0^\infty \widetilde{p}^*(s)\sin(sx)\,ds + \\ + \frac{2\sqrt{2}d_0}{\sqrt{\pi}}\int_0^\infty [\overline{a}_4^*(s)\cos(sx) + f\widehat{a}_4^*(s)\sin(sx)]\widetilde{p}^*(s)\,ds \tag{5.4}$$

We can calculate the first integral from Eq. (5.4) analytically and the second one numerically.

6. Numerical results and discussion

Upon the analysis of the relationship found for calculation of the dimensionless stresses $\sigma_{ij}^{(0)}/p_0$, we conclude that they depend on five non-dimensional parameters: the ratio of the thickness of the top layer and the half-width of contact, the ratio of the layer and Young's moduli of substrates the coefficient of friction and the layer and the substrate Poisson ratios.

In the contact problem for the homogeneous half-space, tensile stresses occur at the trailing edge of the unloaded half-space surface, which was described by Smith and Liu (1953). The maximum value of $\sigma_{xx}^{(0)}/p_0$ occurs at the edge area of contact $(x = -1, z = h)$ and is equal to $8f/\pi$. In the case of the non-homogeneous half-space, tensile stresses in the mentioned zone also appeare (Fig. 4). In that case, mechanical properties of the layer differ insignificantly from the substrate properties, the maximum tensile stress occur at the edge of contact. An increment of the parameter E_0/E_1 causes that the maximum tensile stresses occur in a certain distance from the edge of the contact area. This is more typical for "thick" layers. When the thickness of the layer increases it leads to a decreasing level of dimensionless tensile stresses in the described area.

The second area, in which tensile stresses can occur is the coating/substrate interface (Fig. 4b',c'). In the case of "thin" layers, the tensile stresses in this area do not occur at all or their level is much lower with respect to tensile stresses appearing at the surface. Together with the increasing thickness of the layer or E_0/E_1 parameter, tensile stresses at the interface also increase. For a certain layer thickness, the principal stress σ_1 (we make an assumption that $\sigma_3 < \sigma_2 < \sigma_1$) achieves the largest value at the interface. Figure 5

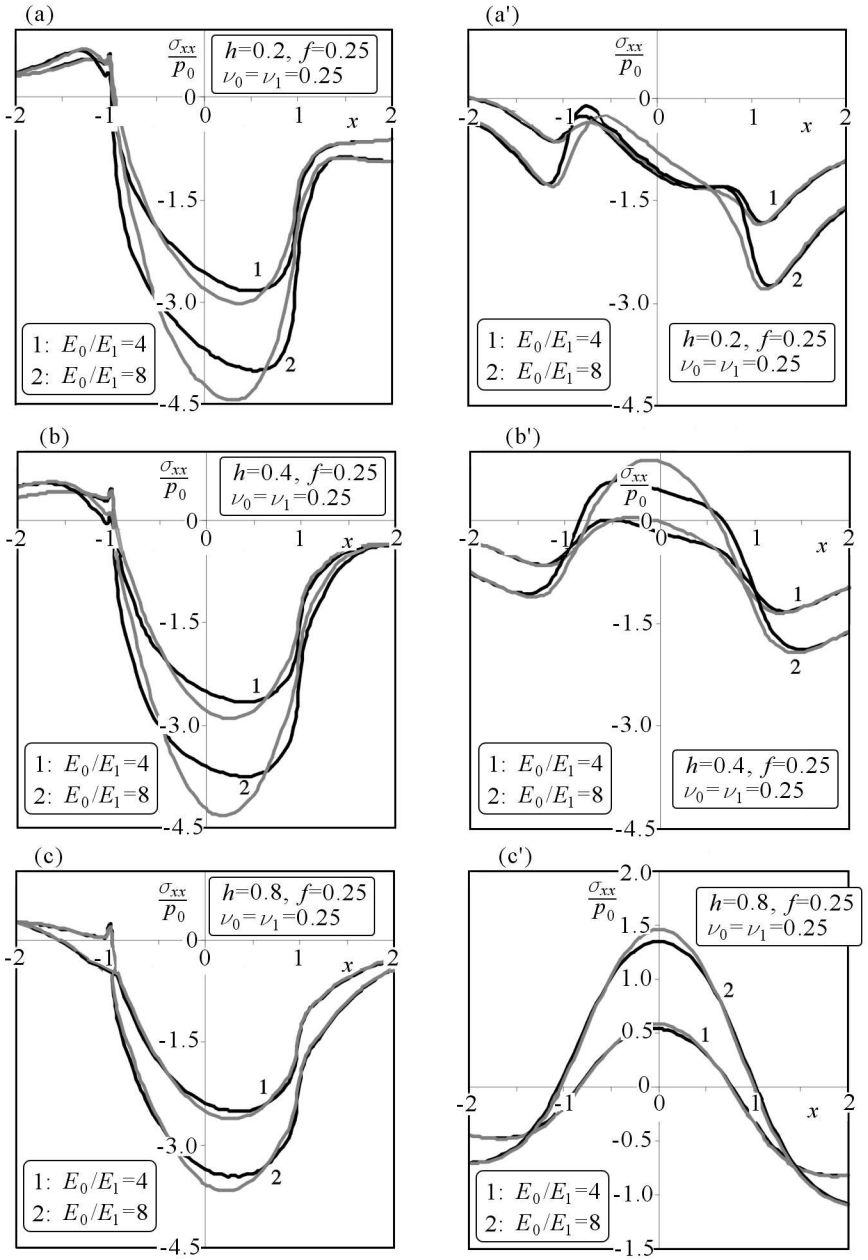

Fig. 4. Distribution of σ_{xx}/p_0 on the non-homogeneous half-space surface (a, b, c) and at the coating/substrate interface (a', b', c'): distribution of the contact pressure on the basis of integral equation (3.6) – black curves, distribution of actual contact pressure replaced by the Hertz solution – gray curve

shows that every curve (except for gray curve 2) consist of two sections. The first section (adequate for smaller values of parameter h) is related with parameters for which the maximum tensile stress occurs on the surface of the non-homogeneous half-space. The second section describes cases in which the maximum tensile stress at the interface is observed. Gray curve 2 shows that an increment in the coefficient of friction can cause that the dominant stress will be stress on the surface of the non-homogeneous half-space.

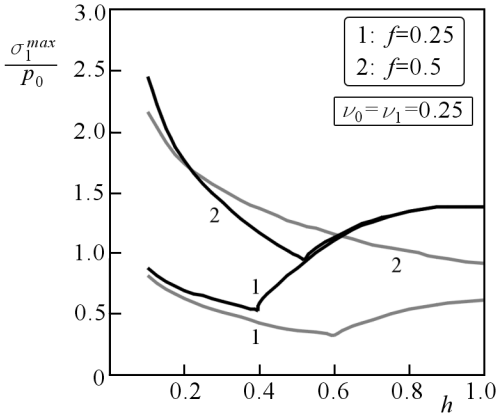

Fig. 5. Relationship between the maximum tensile stresses and non-dimensional layer thickness ($E_0/E_1 = 4$ – gray curves, $E_0/E_1 = 8$ – black curves)

The replacement of the actual contact pressure by Hertz's distribution does not lead to large errors during calculation of the maximum value of the tensile stress on the surface. For the coefficient of friction $f = 0.25$, the calculation error is less than 5%, and for $f = 0.5$ is less than 9% (Fig. 6). In the case of "thin" layers, the error is smaller, and for the thickness $h = 0.2$ is up to 4%.

It is necessary to pay attention to the difference between results described in the present work and results published by Diao *et al.* (1994). The non-dimensional stress distributions $\sigma_{xx}^{(0)}/p_{max}$ on the surface of the half-space calculated on the base of the Hertz contact pressure fully agree with the results published by Diao *et al.* (1994). The difference is included in the parameter p_{max}. In the present paper, the parameter $p_{max} = 4p_0/\pi$ is calculated from the condition of equilibrium of the cylinder. However, in the work by Diao *et al.* (1994), it was assumed that $p_{max} = p_{x=0}$, where $p_{x=0}$ was the actual contact pressure in the centre of the contact area. The value $p_{x=0}$ was taken from the paper by Gupta and Walowit (1974).

The maximum values of tensile stresses at the interface calculated of the basis of the Hertz contact pressure and the distribution of actual pressure considerably differ.

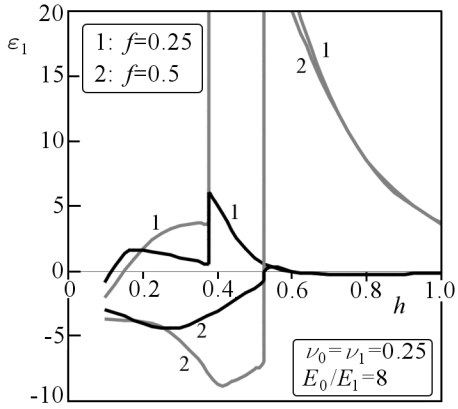

Fig. 6. Error of calculation of the maximum tensile stresses (distribution of pressure replaced by the Hertz solution – gray curves, contact pressure approximated by Eq. (4.1) – black curves)

In the case when $h > 0.2$, the distribution of contact pressure described by Eq. (4.1) permits one to calculate the maximum value of tensile stresses with satisfactory precision both on the surface and at the interface (black curves in Fig. 6).

On the basis of the stress distribution σ_{xx}, it is easy to predict the maximum shear stress distribution in the plane of strain $\tau_1 = \sqrt{(\sigma_{xx} - \sigma_{zz})^2 + 4\sigma_{xz}^2}/2$ and the maximum shear stresses $\tau = (\sigma_1 - \sigma_3)/2$. Calculations confirmed the conclusion of the work by Kouitat Nijwa and von Stebut (1999) that the maximum shear stress τ_1 in the plane of strain assumed the minimal value in the central part of the top layer. The stress τ_1 has the maximal value on the surface of the non-homogeneous half-space (for the determinated level of friction forces or in the case of "thin" layers) or at the coating/substrate interface (for a small coefficient of friction for layers whose thickness exceeds the described value). Moreover, it is necessary to note that the maximum shear stress $\tau = (\sigma_1 - \sigma_3)/2$ is frequently above the maximal value of the stress τ_1. Typical distributions of maximum shear stresses on the surface of the non-homogeneous half-space are shown in Fig. 7. Figure 7 presents that the largest level of the stress τ is achieved in the central part of the contact area $(0 < x < 0.7,\ z = h)$.

In the case of reasonable friction $(f < 0.3)$, the level of maximum shear stresses may be much higher than the level of tensile stresses (Fig. 8).

The error of calculation of the maximum shear stresses due to the replacement of the actual contact pressure by the Hertz pressure may be regarded reasonable (Fig. 9) in the case of "thin" $(h < 0.2)$ and "thick" $(h > 0.7)$ lay-

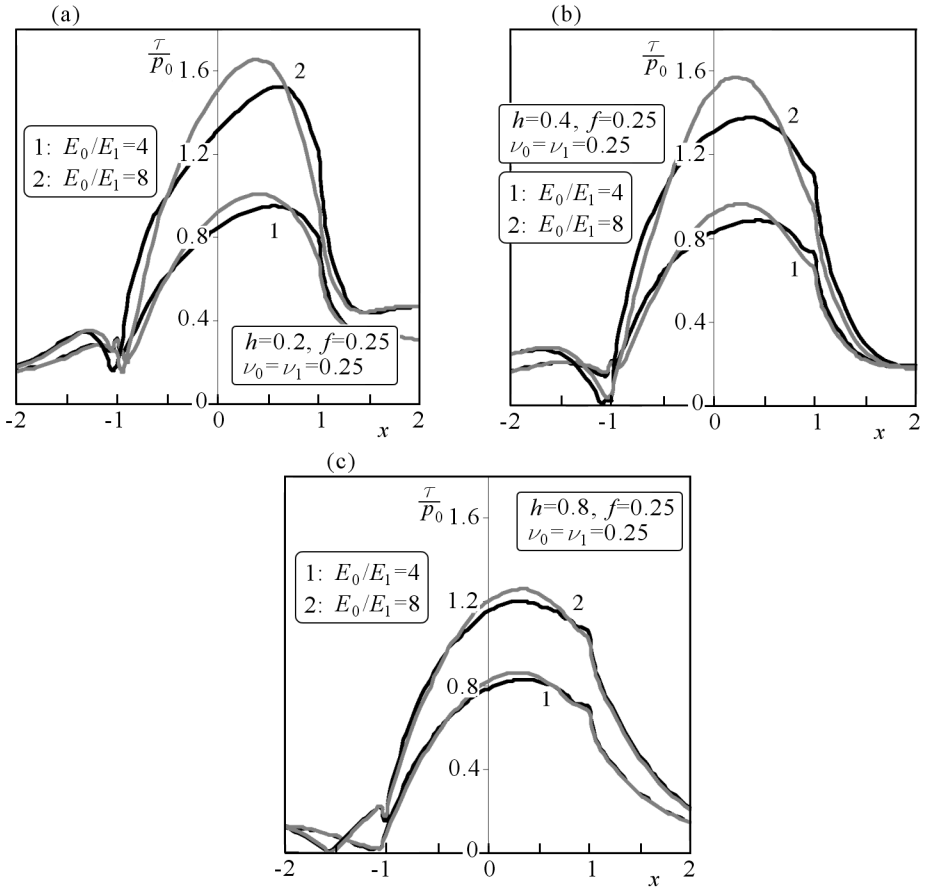

Fig. 7. Distribution of the maximum shear stresses τ/p_0 ($\tau = (\sigma_1 - \sigma_3)/2$) on the surface of the non-homogeneous half-space: contact pressure distribution found from integral equation (3.6) – black curves, distribution of actual contact pressure replaced by the Hertz solution – gray curves

ers. The largest deviation is observed when $h \approx 0.4$. Describing the contact pressure by Eq. (4.1), it permits one to calculate the largest value of the maximum shear stresses with an error up to 3% when $h > 0.3$ (black curves in Fig. 9).

The distribution of shear stresses σ_{xz} at the coating/substrate interface in the case of "thin" layers was described in the paper by Houmid Bennani and Takadoum (1999). A typical distribution, which occurs in the case $h > 0.3$, is shown in Fig. 10. Replacing of the actual contact pressure by the Hertz pressure does not cause considerable changes in the σ_{xz} stress distribution at the coating/substrate interface.

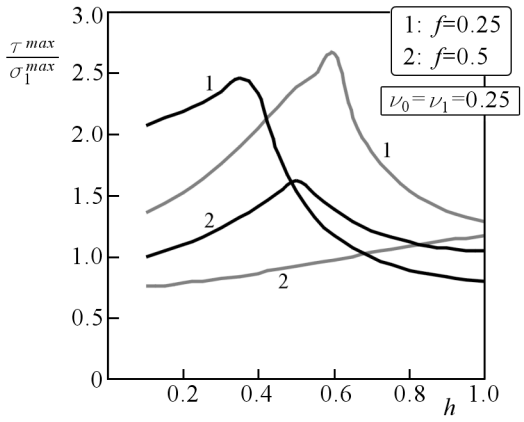

Fig. 8. Relationship between $\tau^{max}/\sigma_1^{max}$ and the non-dimensional layer thickness ($E_0/E_1 = 4$ – gray curves, $E_0/E_1 = 8$ – black curves)

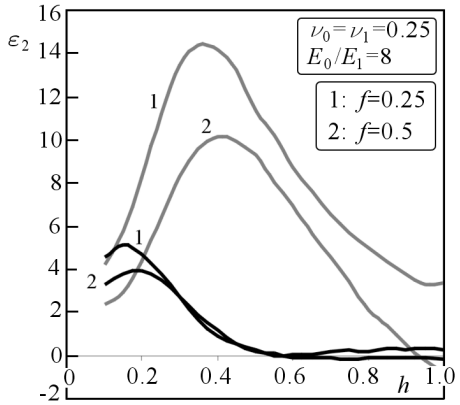

Fig. 9. Calculation error of the maximum τ_1 stresses (distribution of pressure replaced by the Hertz solution – gray curves, contact pressure approximated by Eq. (4.1) – black curves)

7. Conclusions

The analysis of stress distribution in the hard top layer proved that this layer can be divided into three sections: "thin" layers ($h < 0.2$), "thick" layers ($h > 0.7$) and those in between.

In the case of "thin" layers, the maximum tensile stress occurs at the trailing edge of the unloaded half-space surface. The largest value of the tensile stresses can be mostly observed at the edge of the area of contact (except for very large values of the ratio E_0/E_1). The maximum shear stress can turn

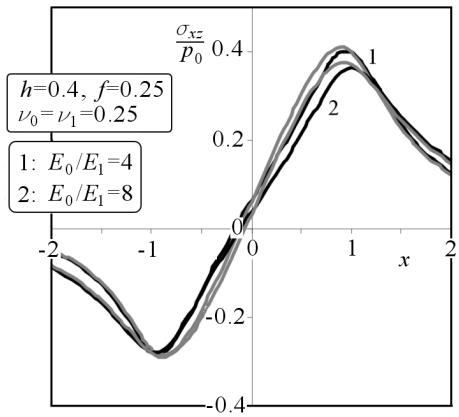

Fig. 10. Typical distribution of σ_{xz}/p_0 stresses at the coating/substrate interface: contact pressure distribution found from integral equation (3.6) – black curves, distribution of actual contact pressure replaced by the Hertz solution – gray curves

out to be much larger (more than twice) from the largest value of the tensile stress. The parameter $\tau^{max}/\sigma_1^{max}$ increases with growing of ratio E_0/E_1 and decreases with growing coefficient of friction. In engineering calculations, we can replace the distribution of actual pressure by the Hertz distribution.

In the case of "thick" layers, the predominant stresses are mostly tensile stresses at the coating/substrate interface (except for very large coefficients of friction). In engineering calculations, we can also apply Hertz distribution.

In the case when $0.2 < h < 0.7$, the maximum tensile stress occurs either at the trailing edge of the unloaded half-space surface or at the coating/substrate interface. In the case of reasonable values of E_0/E_1 and f ($E_0/E_1 < 5$, $f < 0.3$), the parameter $\tau^{max}/\sigma_1^{max}$ is greater than 2. The replacement of the actual contact pressure by the Hertz pressure leads perhaps to larger errors of calculation of the maximum tensile stresses at the coating/substrate interface. The error of calculation of the maximum shear stress often exceeds 10%. In engineering calculations, we can describe the distribution of actual pressure by approximate relation (4.1).

Acknowledgements

The investigation described in this paper is a part of the project W/WM/2/05, funded by the Polish State Committee for Scientific Research and realized at Bialystok University of Technology.

A. Appendix

A system of linear equations for determination of the functions $a_i(s)$, $i = 1, 2, \ldots, 6$ is

$$\mathbf{A}\boldsymbol{a} = \boldsymbol{b} \tag{A.1}$$

where the non-zero elements of the matrix $\mathbf{A}$ are

$$\begin{aligned}
&A_{11} = 2 + d_1 \qquad A_{12} = A_{22} = A_{56} = A_{65} = 2|s| \\
&A_{13} = (2 + d_0)\sinh(|s|h) + d_0|s|h\cosh(|s|h) \\
&A_{14} = (2 + d_0)\cosh(|s|h) + d_0|s|h\sinh(|s|h) \\
&A_{15} = -A_{26} = -A_{36} = A_{45} = 2|s|\cosh(|s|h) \\
&A_{16} = -A_{25} = -A_{35} = A_{46} = 2|s|\sinh(|s|h) \\
&A_{23} = -d_0|s|h\sinh(|s|h) \qquad A_{24} = -d_0|s|h\cosh(|s|h) \\
&A_{31} = \mu^*(1 + d_1) \qquad A_{33} = -(1 + d_0)\cosh(|s|h) - d_0|s|h\sin(|s|h) \\
&A_{32} = 2\mu^*|s| \qquad A_{34} = -(1 + d_0)\sinh(|s|h) - d_0|s|h\cosh(|s|h) \\
&A_{41} = \mu^* \qquad A_{43} = \sinh(|s|h) + d_0|s|h\cosh(|s|h) \\
&A_{42} = 2\mu^*|s| \qquad A_{44} = \cosh(|s|h) + d_0|s|h\sinh(|s|h) \\
&A_{53} = 1 + d_0 \qquad A_{64} = 1 \qquad \mu^* = \frac{\mu_1}{\mu_0}
\end{aligned}$$

and

$$\boldsymbol{b} = \begin{cases} \left[0, 0, 0, 0, 0, \dfrac{1}{\mu_0}\widetilde{p}(s)\right] & \text{problem I} \\ \left[0, 0, 0, 0, -\dfrac{1}{\mu_0} f\widetilde{p}(s)\mathrm{i}\,\mathrm{sgn}\,(s), 0\right] & \text{problem II} \end{cases}$$

B. Appendix

Formulas for calculating parameters A_i and B_i, $i = 1, 2$ are

$$A_1 = \frac{3\pi}{2}\int_0^\infty \overline{a}_6(s)F_1(s)G_1(s)\,ds \qquad A_2 = \frac{9\pi}{2}\int_0^\infty \overline{a}_6(s)F_1(s)G_2(s)\,ds$$

$$B_1 = 8\int_0^\infty \overline{a}_6(s)F_2(s)G_1(s)\,ds \qquad B_2 = 24\int_0^\infty \overline{a}_6(s)F_2(s)G_2(s)\,ds$$

$$F_1(s) = \frac{J_1(s)}{s} - 4\frac{J_2(s)}{s^2} \qquad F_2(s) = \frac{J_1(s)}{s} - 3\frac{J_2(s)}{s^2}$$

$$G_1(s) = \cos s - 1 \qquad G_2(s) = \frac{\sin s}{s} - 1$$

References

1. ANDERSON I.A., COLLINS I.F., 1995, Plane strain stress distributions in discrete and blended coated solids under normal and sliding contact, *Wear*, **185**, 23-33

2. BHOMWICK S., KALE A.N., JAYARAM V., BISWAS S.K., 2003, Contact damage in TiN coatings on steel, *Thin Solid Films*, **436**, 250-258

3. BRAGALLINI G.M., CAVATORTA M.P., SAINSOT P., 2003, Coated contacts: a strain approach, *Tribology International*, **36**, 935-941

4. DIAO D.F., 1999, Finite element analysis on local yield map and critical maximum contact pressure for yielding in hard coating with an interlayer under sliding contact, *Tribology International*, **32**, 25-32

5. DIAO D.F., KATO K., HAYASHI K., 1994, The maximum tensile stress on a hard coating under sliding contact, *Tribology International*, **27**, 4, 267-272

6. EASON G., 1965, The stress produced in a semi-infinite solid by a moving surface force, —em International Journal of Engineering Science, **2**, 581-609

7. ELSHARKAWY A.A., 1999, Effect of friction on subsurface stresses in sliding line contact of multilayered elastic solids, *International Journal of Solids and Structures*, **36**, 3903-3915

8. ELSHARKAWY A.A., HAMROCK B.J., 1993, A numerical solution for dry sliding line contact of multilayered elastic bodies, *Journal of Tribology*, **115**, 237-245

9. GALIN L.A., 1980, *Contact Problems in the Theory of Elasticity and Viscoelasticity*, Nauka, Moscow

10. GUPTA P.K., WALOWIT J.A., 1974, Contact stresses between an elastic cylinder and a layered elastic solid, *Journal of Lubrication Technology*, **96**, 250-257

11. GUPTA P.K., WALOWIT J.A., FINKIN E.F., 1973, Stress distributions in plane strain layered elastic solids subjected to arbitrary boundary loading, *Journal of Lubrication Technology*, 427-433

12. HOUMID BENNANI H., TAKADOUM J., 1999, Finite element model of elastic stresses in thin coatings submitted to applied forces, *Surface and Coatings Technology*, **111**, 80-85

13. JOHNSON K.L., 1985, *Contact Mechanics*, Cambridge University Press, Cambridge

14. KATO K., 2000, Wear in relation to friction – a review, *Wear*, **241**, 151-157

15. KOUITAT NJIWA R., CONSIGLIO R., VON STEBUT J., 1998, Boundary element modelling of coated materials in static and sliding ball-flat elastic contact, *Surface and Coatings Technology*, **102**, 148-153

16. KOUITAT NIJWA R., VON STEBUT J., 1999, Boundary element numerical modelling as a surface engineering tool: application to very thin coatings, *Surface and Coatings Technology*, **116/119**, 573-579

17. SCHWARZER N., 2000, Coating desing due to analytical modelling of mechanical contact problems on multilayer systems, *Surface and Coatings Technology*, **133/134**, 397-402

18. SMITH J.O., LIU C. K., 1953, Stresses due to tangential and normal loads on an elastic solid with application to some contact stress problems, *Journal of Applied Mechanics*, **20**, 157-166

19. XIE C., TONG W., 2005, Cracking and decohesion of a thin Al_2O_3 film on a ductile Al-5%Mg substrate, *Acta Materialia*, **53**, 477-485

Naprężenia w twardej warstwie wierzchniej wywołane obciążeniami kontaktowymi

Streszczenie

Rozpatrzono dwuwymiarowe zagadnienie kontaktowe teorii sprężystości dotyczące wciskania nieodkształcalnego walca w półprzestrzeń sprężystą pokrytą sprężystą warstwą. Przeprowadzono szczegółową analizę rozkładu naprężeń wywołanego naciskami kontaktowymi i powiązanymi z nimi siłami tarcia. Otrzymane wyniki porównano z wynikami, które otrzymuje się w zagadnieniu teorii sprężystości dotyczącym obciążenia powierzchni rozpatrywanej półprzestrzeni niejednorodnej naciskami Hertza.

Manuscript received January 26, 2007; accepted for print March 26, 2007